HIV-1 Vpr-Induced Apoptosis Is Cell Cycle Dependent and Requires Bax but Not ANT

Joshua L. Andersen[1], Jason L. DeHart[1], Erik S. Zimmerman[1], Orly Ardon[1], Baek Kim[2], Guillaume Jacquot[3], Serge Benichou[3], Vicente Planelles[1*]

1 Department of Pathology, University of Utah School of Medicine, Salt Lake City, Utah, United States of America, **2** Department of Microbiology and Immunology, University of Rochester Medical Center, Rochester, New York, United States of America, **3** Departement de Maladies Infectieuses, Institut Cochin, Institut National de la Santé et de la Recherche Médicale, Paris, France

The HIV-1 accessory protein viral protein R (Vpr) causes G_2 arrest and apoptosis in infected cells. We previously identified the DNA damage–signaling protein ATR as the cellular factor that mediates Vpr-induced G_2 arrest and apoptosis. Here, we examine the mechanism of induction of apoptosis by Vpr and how it relates to induction of G_2 arrest. We find that entry into G_2 is a requirement for Vpr to induce apoptosis. We investigated the role of the mitochondrial permeability transition pore by knockdown of its essential component, the adenine nucleotide translocator. We found that Vpr-induced apoptosis was unaffected by knockdown of ANT. Instead, apoptosis is triggered through a different mitochondrial pore protein, Bax. In support of the idea that checkpoint activation and apoptosis induction are functionally linked, we show that Bax activation by Vpr was ablated when ATR or GADD45α was knocked down. Certain mutants of Vpr, such as R77Q and I74A, identified in long-term nonprogressors, have been proposed to inefficiently induce apoptosis while activating the G_2 checkpoint in a normal manner. We tested the in vitro phenotypes of these mutants and found that their abilities to induce apoptosis and G_2 arrest are indistinguishable from those of HIV-1_{NL4-3} *vpr*, providing additional support to the idea that G_2 arrest and apoptosis induction are mechanistically linked.

Citation: Andersen JL, DeHart JL, Zimmerman ES, Ardon O, Kim B, et al. (2006) HIV-1 Vpr-induced apoptosis is cell cycle dependent and requires Bax but not ANT. PLoS Pathog 2(12): e127. doi:10.1371/journal.ppat.0020127

Introduction

Loss of $CD4^+$ lymphocytes is a hallmark of progression to acquired immune deficiency syndrome (AIDS). The mechanisms proposed to explain the loss and dysfunction of $CD4^+$ T cells are multiple and include indirect effects of viral infection, such as generalized activation of the immune system, $CD8^+$ cytotoxic T lymphocyte–mediated killing of infected cells, as well as direct effects of infection such as virus budding, and expression of certain viral genes (reviewed in [1–3]). Analysis of virus dynamics in vivo has revealed that a significant portion of $CD4^+$ T-cell death is due to virus-induced cytotoxicity in the infected cells [4–6], and the estimated half-life of infected lymphocytes is on the order of 2 d (reviewed in [7]). Therefore, studies that seek to understand the molecular and cellular basis of HIV-1–induced death in T cells are critical toward explaining how immune deterioration results from HIV-1 infection.

The HIV-1 viral protein R (Vpr) has emerged as a major proapoptotic gene product (reviewed in [8,9]). In an effort to characterize the apoptotic signaling cascade induced by Vpr downstream of the mitochondria, Muthumani et al. [10,11] demonstrated that Vpr induces apoptosis via the intrinsic pathway. This pathway is characterized by cytochrome *c* release and caspase 9 activation and is triggered in the absence of death receptor ligation.

Vpr induces a second type of cytopathic effect by blocking the cell cycle in the G_2 phase. We, and others, have previously shown that Vpr causes activation of the G_2 checkpoint protein, ATR (ataxia and telangiectasia mutated and Rad3 related), a serine/threonine kinase responsive to DNA damage and replication stress [12–14]. Furthermore, activation of ATR by Vpr is required for Vpr-induced G_2 arrest and involves the ATR-associated molecules Rad17 and the Rad9-Rad1-Hus1 trimer [14–16].

A cause–effect relationship between the two deleterious actions of Vpr (G_2 arrest and apoptosis) has not been established. Indirect evidence supports the notion that induction of G_2 arrest and apoptosis are linked. For example, treatment of cells with either caffeine, an inhibitor of ATR/ATM checkpoint function, or small interfering RNA (siRNA) specific to ATR, relieves both Vpr-induced G_2 arrest and apoptosis [17,18]. In addition, Yuan et al. [19,20] demonstrated that siRNA knockdown of Wee1, a Cdk1 inhibitor that is activated by DNA damage, abrogated both Vpr-induced G_2 arrest and apoptosis. Taken together, these data suggest a model in which checkpoint activation and apoptosis signaling

Editor: Michael Malim, King's College London, United Kingdom

Received May 11, 2006; **Accepted** October 25, 2006; **Published** December 1, 2006

Abbreviations: ANT, adenine nucleotide transporter; ATM, ataxia telangiectasia mutated; ATR, ataxia and telangiectasia mutated and Rad3 related; BRCA1, breast cancer–associated protein 1; DAPI, 4′,6-diamidino-2-phenylindole dihydrochloride; DSB, double-strand break; GADD45α, growth arrest and DNA damage–responsive protein α; GFP, green fluorescent protein; HIV-1, human immunodeficiency virus type 1; MNNG, *N*-methyl-*N*′-nitro-*N*-nitrosoguanidine; mRFP, monomeric red fluorescent protein; PARP, poly-ADP-ribose polymerase; PTPC, permeability transition pore complex; siRNA, small interfering RNA; Smac, second mitochondria-derived activator of caspase; VDAC, voltage-dependent anion channel; Vpr, viral protein R

* To whom correspondence should be addressed. E-mail: Vicente.planelles@path.utah.edu

Synopsis

HIV-1 encodes a small gene known as *vpr* (viral protein regulatory) whose product is a 96–amino acid protein. HIV-1 infects cells of the immune system, such as CD4-positive lymphocytes. When cells become infected with HIV-1, two deleterious effects result from expression of the *vpr* gene. One effect of *vpr* is to manipulate the cell cycle by blocking the cells in G_2 (the phase of the cell cycle immediately preceding mitosis). Thus, cells infected with HIV-1 cease to proliferate, due to the action of *vpr*. A second effect of *vpr* is the induction of cell death by a process known as apoptosis or programmed cell death. When cells die by apoptosis, they do so following activation of a cellular set of genes and proteins whose primary function is to inactivate various cellular functions that are needed in order to maintain cellular viability. In this study, Andersen et al. demonstrate that the above two effects of *vpr* are linked. In particular, the authors show that the blockade in cell proliferation in G_2 is a requirement toward the onset of programmed cell death. Programmed cell death can be accomplished by a number of cellular proteins known as "executioners." Various executioner proteins reside on the mitochondrial membranes and may trigger release of factors from the mitochondria, which in turn will precipitate the onset of apoptosis. In this work Anderson et al. identify the mitochondrial protein, Bax, as the key executioner of apoptosis in the context of HIV-1 *vpr*. The authors' findings provide important mechanistic understanding of how the *vpr* gene contributes to HIV-1–induced cell death.

by Vpr are functionally associated and that such an association stems from the ability of Vpr to activate ATR [12–14,17].

On the other hand, evidence from mutagenesis studies suggests that checkpoint activation and apoptosis may be separable effects of Vpr. Thus, mutants of Vpr have been described that induce normal levels of G_2 arrest but are partially impaired for induction of apoptosis [21,22]. One model to explain the proapoptotic activity of Vpr was proposed by Jacotot et al. [23] and Vieira et al. [24], who observed that recombinant Vpr associates with the adenine nucleotide transporter (ANT) on purified mitochondria, to directly promote release of mitochondrion-associated cytochrome *c* and apoptosis. This finding suggested that Vpr initiated the commitment to apoptosis at the mitochondrial membrane by binding to ANT, rather than by activating upstream stress signaling pathways derived from checkpoint activation.

In the present study, we examine the relationship between induction of G_2 arrest and onset of apoptosis by Vpr. We find that entry into G_2 is a requirement for Vpr to induce apoptosis. Since the requirement for entry into G_2 seemed inconsistent with the reported ability of Vpr to bind to ANT and promote apoptosis in a cell cycle–independent manner, we then examined the requirement for ANT. We find that Vpr-induced apoptosis is unaffected by knockdown of ANT. Instead, Vpr-induced apoptosis is dependent on the presence of Bax and is concomitant with Bax activation. Furthermore, Bax activation is a result of proapoptotic signals transduced by Vpr through the upstream stress proteins ATR and GADD45α (growth arrest and DNA damage–responsive protein α) because knockdown of ATR or GADD45α prevented activation of Bax. We also demonstrate that, despite the striking similarities between the signaling events induced by Vpr and those induced by genotoxic stress, important differences can be found. Specifically, Vpr-induced apoptosis is abrogated by checkpoint inhibition, while apoptosis induced by genotoxic agents is exacerbated by checkpoint inhibition. Taken together, these results demonstrate that Vpr activates the ATR-initiated DNA damage–signaling pathway to link checkpoint activation and commitment to apoptosis.

Results

G_2 Arrest Precedes the Release of Mitochondrial Smac and Caspase Activation

Treatment with caffeine, an inhibitor of ATR and ATM, or siRNA targeted to ATR, abrogates Vpr-induced G_2 arrest and apoptosis [14,17,18]. One possible explanation for these observations would be that Vpr induces apoptosis as a downstream consequence of sustained G_2 checkpoint activation. This idea, however, is inconsistent with a previously published model in which Vpr was proposed to directly bind to the mitochondrial ANT to cause release of proapoptotic factors in a cell cycle–independent manner [23,24].

To begin to differentiate between these models, we studied the kinetics of induction of G_2 arrest and apoptosis. If apoptosis were a consequence of G_2 checkpoint signaling, we would predict that G_2 arrest should precede the onset of apoptosis. However, if Vpr were binding ANT to induce apoptosis, we would predict that commitment to apoptosis should be independent of cell cycle status and would occur early following expression of Vpr. We transduced a human $CD4^+$ T-lymphocyte cell line, SupT1, with lentiviral vectors (pHR-VPR-G or pHR-VPR-R) expressing Vpr and either green fluorescent protein (GFP) or monomeric red fluorescent protein (mRFP), respectively, with an intervening internal ribosome entry site (Figure 1A). Having essentially identical vectors with different fluorescent tags allowed us to stain infected cells with a variety of fluorescent indicators of cell cycle profile and apoptosis. As a control, we used isogenic vectors expressing a mutant form of Vpr, pHR-VPR(R80A), wherein Vpr(R80A) is defective in induction of G_2 arrest and apoptosis [17,25–27]. These vectors were previously described in detail [13,17,26]. In parallel experiments, we transduced SupT1 cells with VSV-G pseudotyped, env-defective vector derived from HIV-1_{NL4-3} (DHIV3; Figure 1A) or a mutant form of the previous vector with Vpr deleted (DHIV3-ΔVPR). At various time points, cultures were harvested and partitioned for further analyses. Analyses included cell cycle profile, induction of apoptosis as measured by caspase activation, and Western blot to detect release of Smac (second mitochondria-derived activator of caspase) into the cytoplasm.

Accumulation of Vpr-expressing cells at G_2 began at 24 h post-transduction, peaked at 48 h, and persisted throughout the remainder of the experiment (Figure 1B). In contrast, caspase activation in Vpr-expressing cells was first detected at 36 h and continued to increase throughout the remainder of the experiment (Figure 1C). Release of Smac (Figure 1D) also occurred late, between 72 and 96 h post-transduction. Samples of flow cytometry charts from experiments shown in Figure 1C at the 72-h time point are presented in Figure 1E.

Therefore, induction of G_2 arrest is an early Vpr-mediated event, whereas release of Smac and caspase activation lag in

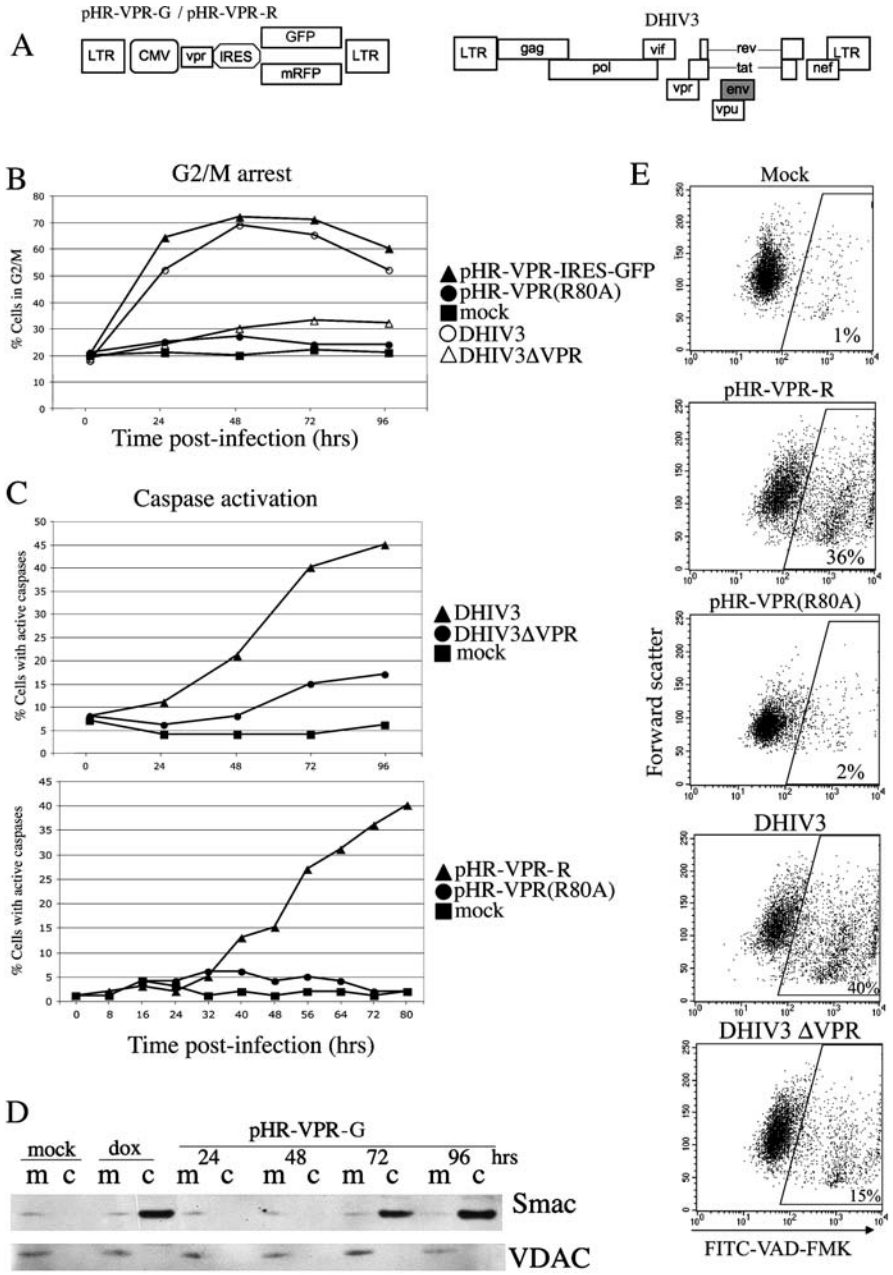

Figure 1. Vpr-Induced Caspase Activation and Smac Release from the Mitochondria Are Temporally Delayed in Relation to G_2 Arrest

(A) pHR-VPR-G and pHR-VPR-R are bicistronic lentiviral vectors that encode HIV-1_{NL4-3} *vpr*, an internal ribosome entry site, and either the gene for GFP or that for mRFP, respectively; pHR-VPR(R80A) was derived from pHR-VPR (both the mRFP and the GFP versions) by site-directed mutagenesis; DHIV3 is an envelope-truncated (see gray box) version of HIV-1_{NL4-3}; DHIV3-ΔVPR was derived from DHIV-3 by introducing a frameshift mutation in *vpr*.

(B) SupT1 T lymphocytes were transduced by spin-infection in the presence of 10 μg/ml Polybrene with indicated vectors. Mock-infected cells were subjected to spin-infection in the presence of 10 μg/ml Polybrene without virus. Cells were collected at specified time points post-transduction, stained with propidium iodide, and analyzed for DNA content by flow cytometry to determine cell cycle profiles. The percentage of cells transduced with pHR vectors and DHIV3 viruses ranged between 70% to 80% and between 65% to 70%, respectively, as determined by mRFP or GFP expression (with pHR vectors) or intracellular p24 staining (with DHIV3 vectors).

(C) Caspase activation was measured as an indication of apoptosis. SupT1 cells were infected with indicated vectors, harvested, and incubated with FITC-VAD-FMK. The percentage of caspase-active cells at each time point was measured by flow cytometry.

(D) Infected SupT1 cells were lysed, and lysates were fractionated into mitochondrial (m) and cytoplasmic (c) fractions and then assayed by Western blot. Western blots were probed with antibodies specific to Smac to measure release from mitochondria and with anti-VDAC antibodies to measure mitochondrial contamination in the cytoplasmic fractions. As a positive control for apoptosis, SupT1 cells were treated with 0.8 μg/ml doxorubicin (dox) for 48 h.

(E) Examples of flow cytometric analysis of caspase activation, corresponding to the 72-h time points from (C).

doi:10.1371/journal.ppat.0020127.g001

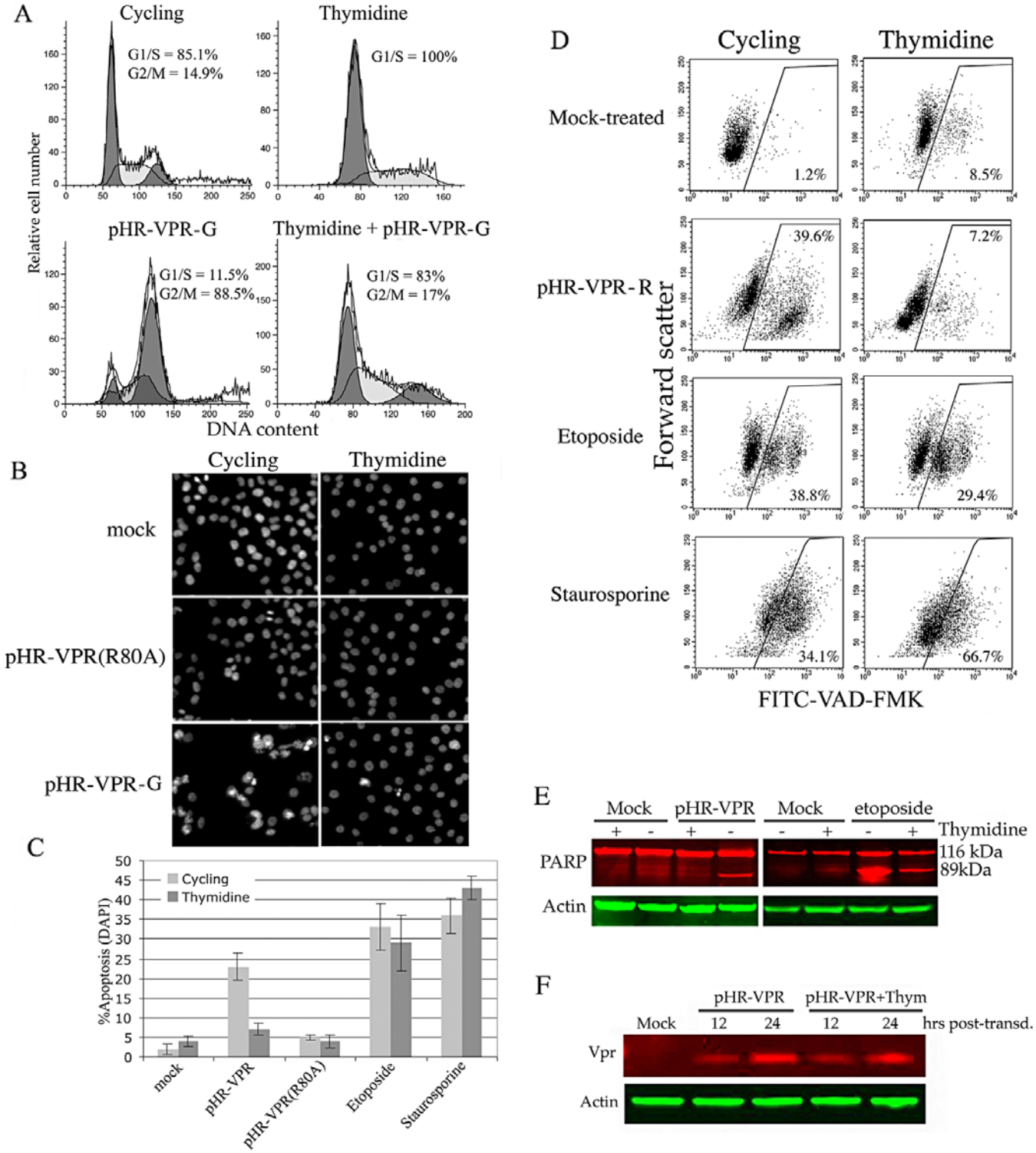

Figure 2. The Apoptotic Effect of Vpr Is Lost in Cells Synchronized in G_1/S

(A) HeLa cells were transduced with pHR-VPR-G or mock-transduced and then incubated with 2 mM thymidine. After 24 h of incubation, cells were harvested, stained with PI, and analyzed for DNA content by flow cytometry to determine the percentage of cells in G_1/S and G_2/M. Transduction efficiency of pHR-VPR in both thymidine-treated and cycling cells was 70% to 75% as determined by analysis of GFP expression by flow cytometry (unpublished data).
(B) Cells from experiments shown in (A) were stained for DAPI at 72 h postinfection, in order to evaluate apoptosis via chromatin morphology
(C) Quantitation of apoptosis in DAPI-stained samples shown in (B); incubation with 25 μM etoposide for 48 h or 1 μM staurosporine for 8 h was included in both cycling and thymidine-treated cells, for comparative purposes.
(D) Cycling or thymidine-synchronized HeLa cells were mock-transduced or transduced with either pHR-VPR-R or pHR-VPR(R80A) for apoptosis analysis, using FITC-VAD-FMK. As positive controls for apoptosis, cycling and synchronized cells were treated with etoposide or staurosporine as shown in (C).
(E) Cycling or thymidine-synchronized HeLa cells expressing Vpr or treated with 25 μM etoposide for 48 h were lysed and analyzed by Western blot for PARP cleavage as a marker of apoptosis/caspase activity. The caspase-cleaved PARP band is observed at 89 kDa.
(F) Cell lysates from pHR-VPR–transduced cells, with or without thymidine block, were harvested at 12 and 24 h post-transduction and analyzed by Western blot for Vpr expression with antibodies specific to the amino-terminal hemagglutinin tag.
doi:10.1371/journal.ppat.0020127.g002

relation to cell cycle arrest by approximately 24 h. Since G_2 arrest clearly precedes apoptosis, we found it compelling to ask whether transition into G_2 was required for the commitment to apoptosis in Vpr-expressing cells.

G_1/S Block Abolishes the Induction of Apoptosis by Vpr

We designed an experiment to prevent Vpr-expressing cells from entering G_2 and then asked whether these cells would still be susceptible to Vpr-induced apoptosis. We chose to perform the experiment in HeLa cells since these cells can be synchronized by incubation with 2 mM thymidine with minimal toxicity [28]. HeLa cells represent an appropriate cell type to study Vpr-induced apoptosis, because ATR activation, breast cancer–associated protein 1 (BRCA1) phosphorylation, and GADD45α upregulation are conserved from HeLa cells to primary human $CD4^+$ lymphocytes [14,17,26,29]. HeLa cells were transduced with pHR-VPR-G and, 4 h later, treated with 2 mM thymidine, which arrests cells at the G_1/S boundary [28]. DNA content analysis showed that thymidine treatment effectively synchronized uninfected cells in G_1/S (Figure 2A). Thymidine synchronization of pHR-VPR-G–infected cells resulted in 82.9% cells in G_1/S and 17.0% cells in G_2/M. The comparatively high number of cells in G_2/M in the synchronized, pHR-VPR–infected culture (17%) reflects cells that reached G_2/M prior to synchronization and arrested due to Vpr expression. To evaluate the frequency of apoptotic cells in these cultures, cells were stained with the nuclear dye 4′,6-diamidino-2-phenylindole dihydrochloride (DAPI). DAPI binds to chromatin and reveals the presence of a conspicuous pyknotic nuclear morphology that is associated with late stages of apoptosis. We have previously described the use of DAPI for analysis of Vpr-induced apoptosis [17,30]. Figure 2B shows fluorescence microscopy photographs from this analysis, and quantitations are shown in Figure 2C. DAPI staining revealed that at 48 h post-transduction, 23% of cells transduced with Vpr were apoptotic if allowed to cycle, whereas only 7% were apoptotic if treated with thymidine (Figure 2C). The background level of apoptosis in uninfected cells treated with thymidine was 4%.

To address whether the decreased sensitivity of G_1/S-arrested cells to Vpr-induced apoptosis could be due to thymidine treatment itself, cells were treated with a pharmacologic apoptosis inducer (etoposide or staurosporine) and then allowed to cycle, or not (thymidine incubation). Staurosporine is a kinase inhibitor and potent inducer of apoptosis with no known cell cycle specificity. Etoposide is a topoisomerase II inhibitor and an inducer of double-strand breaks (DSBs) and, like Vpr, causes G_2 arrest [31,32]. Treatment with staurosporine or etoposide effectively induced apoptosis in both G_1/S-arrested and cycling cells (Figure 2C).

To confirm the previous apoptosis results, we performed parallel experiments using pHR-VPR-R and staining for caspase activity with FITC-VAD-FMK (Figure 2D) and by measuring poly-ADP-ribose polymerase (PARP) cleavage (Figure 2E). Analysis of Vpr expression by Western blot revealed that thymidine treatment did not affect expression of Vpr (Figure 2F). These results are in agreement with those obtained by DAPI staining and confirm that synchronization of cells in G_1/S alleviates Vpr-induced apoptosis.

Release of Vpr-Expressing Cells from G_1/S Block Leads to G_2 Arrest-Dependent Apoptosis

The previous results indicate that the proapoptotic effect of Vpr is lost when cells are artificially maintained in G_1/S. To determine whether induction of apoptosis by Vpr specifically requires transition into G_2, cells were synchronized as in the previous experiment and then were released from thymidine block and allowed to reenter the cell cycle. Released cells were harvested at specified intervals to examine cell cycle progression (Figure 3A) and apoptosis (Figure 3B). Both mock-treated and Vpr-expressing cells entered G_2 at 12 h postrelease. Mock-infected cells completed the first division cycle at 18 h postrelease and continued to cycle (Figure 3A, upper panels), while cells expressing Vpr persisted in G_2 for the remainder of the experiment (Figure 3A, lower panels). A small amount of cells (17.4%) in the Vpr-transduced culture reached G_1 at 18 h postrelease. The reason for this is that the efficiency of transduction with pHR-VPR was about 80% and therefore about 20% are untransduced.

We then asked when, after release from the thymidine block, Vpr-expressing cells would enter apoptosis. Cells which were synchronized, maintained in G_1 for 48 h, and then released (Figure 3B, lanes 2–6) began to display detectable PARP cleavage by 12 h postrelease (Figure 3B, lane 3). Therefore, the onset of apoptosis in Vpr-expressing cells is concomitant with entry into the G_2 phase. In the absence of synchronization in G_1 (Figure 3B, lanes 7–11), Vpr-expressing cells begin to display PARP cleavage by 24 h post-transduction. Synchronized cells, in the absence of Vpr expression, did not display PARP cleavage after release (unpublished data).

Parallel samples from the previous synchronization experiment were also analyzed by DAPI staining (Figure 3C). These experiments revealed chromatin fragmentation/condensation in Vpr-expressing cells at 24 and 48 h postrelease (Figure 3C).

Taken together, these data indicate that Vpr-induced apoptosis requires entry into the G_2 phase and artificially maintaining cells in G_1 effectively prevents the onset of apoptosis.

Inhibition of ATR Prevents Vpr-Induced Apoptosis but Exacerbates Genotoxin-Induced Apoptosis

Due to the phenotypic similarities between Vpr and genotoxic stress, many studies on Vpr have been modeled based on the current understanding of DNA damage signaling [12,14,33]. Several reports have shown that suppression of G_2 checkpoint-activating kinases after exposure to genotoxic agents overrides cell cycle arrest but exacerbates apoptosis [34–37]. The reason for this increase in cell death is thought to be the inability of cells to successfully duplicate DNA or to align and segregate damaged chromosomes during mitosis (reviewed in [35]). Thus, we set out to compare in parallel the effect of ATR suppression on Vpr- versus genotoxin-induced apoptosis. We reasoned that if Vpr causes irreparable DNA damage, then the effect of checkpoint overriding on Vpr-induced apoptosis should mirror that of cells treated with genotoxic agents. To test this, we treated cells with siRNAs specific to ATR, ATM, or nonspecific siRNA. At 48 h following siRNA transfection, we treated cells with 25 μM *N*-methyl-*N*′-nitro-*N*-nitrosoguanidine (MNNG), an SN1-type methylating agent and inducer of G_2 arrest, or 25 μM etoposide. At 24- and 48-h time points following the addition

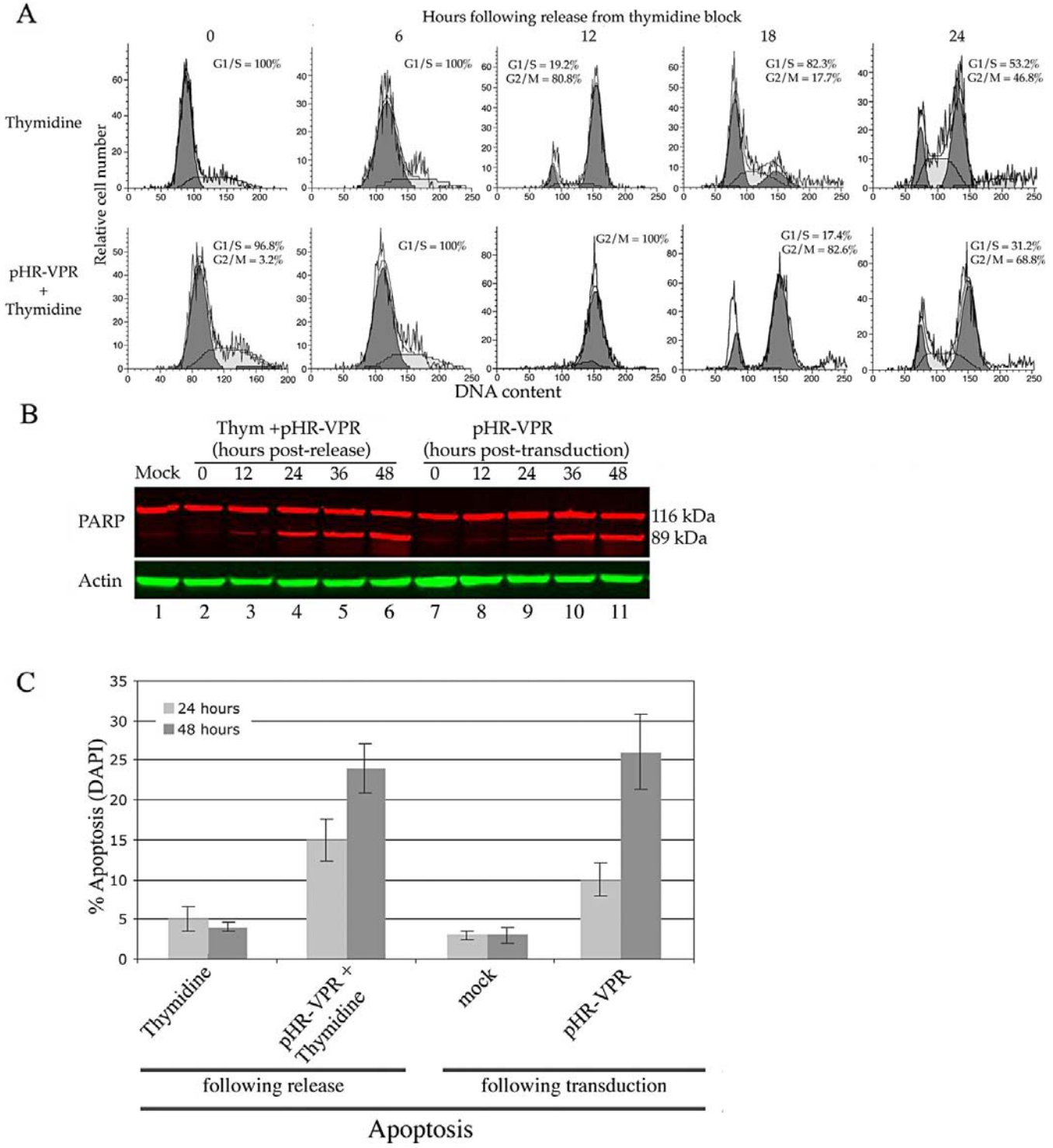

Figure 3. Release of Vpr-Expressing Cells from Thymidine Block Leads to Reentry into the Cell Cycle and Vpr-Induced, G_2-Dependent Apoptosis

(A) Thymidine-synchronized HeLa cells transduced with pHR-VPR-G or mock-transduced were released from thymidine block and harvested at specified time points postrelease. Cells from each time point were stained with PI and analyzed for DNA content by flow cytometry.

(B) pHR-VPR–transduced HeLa cells from the same experiment were monitored by Western blot for PARP cleavage at specified time points. Time points labeled under "Thym + pHR-VPR" indicate hours following release from thymidine block; time points under "pHR-VPR" indicate hours following transduction, as these cells were not synchronized.

(C) Cells treated as those in (A) and (B) were harvested at 24 and 48 h were analyzed for apoptosis by DAPI staining, and the results are quantified.

doi:10.1371/journal.ppat.0020127.g003

of etoposide or MNNG, we measured caspase activation (Figure 4A and 4B; for simplicity, only one time point is shown in 4A). Knockdown of ATR dramatically exacerbated etoposide- and MNNG-induced apoptosis (14.5% to 60.7% and 6.2% to 35.4%, respectively, at 48 h). Knockdown of ATM led to a modest increase in genotoxin-induced apoptosis (14.5% to 21.3% for etoposide and 6.2% to 10% for MNNG, at 48 h). In contrast, Vpr-induced caspase activation was dramatically inhibited by ATR knockdown (from 41.2% to 14.2%) but was unaffected by ATM knockdown (41.2% to 39.4%). DAPI staining showed a similar ATR-dependent decrease in Vpr-induced apoptosis (Figure 4C). The level of knockdown achieved by each siRNA was determined by Western blot with antibodies specific for the endogenous proteins (Figure 4D).

In conclusion, we demonstrated the requirement for ATR checkpoint activation through two different methodologies: (a) manipulation by G_1/S synchronization and (b) ATR knockdown. We also conclude that this aspect of Vpr function represents a departure from the manner in which checkpoint activation relates to apoptosis in the context of genotoxic agents.

Vpr-Induced Apoptosis Does Not Require ANT but Is Mediated via Bax, Downstream of ATR Activation

Early reports suggested that the permeability transition pore complex (PTPC), which consists of VDAC, ANT, and cyclophilin D, was involved in release of apoptotic factors from the mitochondria in response to various apoptotic stimuli (reviewed in [38]) and, in particular, for Vpr [23]. However, later reports have put in question the role of the PTPC in DNA damage–induced apoptosis [39–42]. For example, mouse cells deficient in ANT are fully capable of undergoing apoptosis in response to DNA damage and, instead, show increased resistance to necrosis in response to high intracellular Ca^{2+} [39]. Mouse cells deficient in cyclophilin D, which is required for VDAC function, are fully capable of undergoing apoptosis in response to genotoxins [40,42]. Large oligomeric complexes containing Bax and possessing apoptotic pore function do not contain ANT or VDAC [43]. Bax is required for activation of the mitochondrial pore-forming complex that responds to DNA damage (reviewed in [44,45]) and the pore-forming function of Bax is independent of ANT or VDAC [43,46–48].

Thus, we asked whether Vpr-induced apoptosis is mediated through ANT or, alternatively, through Bax. We addressed this question using siRNAs that would specifically downregulate Bax or ANT, in the context of pHR-VPR-R transduction. Bax knockdown led to a dramatic decrease in Vpr-induced apoptosis (from 41.2% in the presence of nonspecific siRNA to 12.6% in the presence of Bax siRNA; Figure 4A), whereas ANT knockdown had no appreciable effect on apoptosis (41.2% versus 39.5%; Figure 4A). These results were also confirmed by analysis of DAPI-stained nuclei (Figure 4C). The levels of knockdown achieved by each siRNA are shown in Figure 4D.

Activation of Bax is associated with a conformational change that exposes an N- terminal epitope detected by monoclonal antibody Bax6A7 [49]. Thus, reactivity with Bax6A7 provides a direct measurement of Bax activation. To probe for Bax activation in the presence of Vpr, peripheral blood $CD4^+$ lymphocytes were infected with either DHIV3 or DHIV3-ΔVPR, cells were lysed, and immunoreactivity with Bax6A7 antibody was tested by immunoprecipitation followed by Western blot (Figure 4E). Reactivity with Bax6A7 was increased following infection with DHIV3, when compared with that of mock- or DHIV3-ΔVPR–infected cells.

Our previous studies established that Vpr-induced ATR activation leads to BRCA1 phosphorylation and GADD45α upregulation and that both ATR and GADD45α are required for Vpr-induced apoptosis [14,17]. Based on previous findings and data reported here, we propose that ATR activation is an upstream signaling event in the pathway leading to Vpr-induced cell cycle arrest and apoptosis. If this were correct, then it would follow that Bax activation by Vpr is also ATR dependent. In order to examine the requirement of ATR in Vpr-induced Bax activation, we treated cells with siRNAs specific to either ATR or GADD45α prior to transduction with pHR-VPR-R. We observed that the increase in Bax6A7 reactivity was reduced to basal levels in the presence of either ATR or GADD45α knockdown but not when using a nonspecific siRNA (Figure 4F). Therefore, these results provide additional support for a model in which Bax activation is a principal effector of Vpr-induced apoptosis downstream of G_2 checkpoint activation by the ATR kinase.

Effect of Vpr on Mitotic Entry

It is unclear whether cells arrested in G_2 by Vpr transition into mitosis. Early measurements of the mitotic index suggested that Vpr induced G_2 arrest and concomitantly inhibited entry into mitosis [50–53]. Later studies, however, showed that cells expressing Vpr develop mitotic abnormalities such as multipolar spindles, mislocalization of certain spindle pole body proteins, and defects in cytokinesis [54,55], collectively indicating mitotic entry. To reexamine the issue of mitotic entry in the context of Vpr, we measured phosphorylation of histone 3 (H3) at serine-10 [56,57] in the presence of Vpr (Figure 5). As positive and negative controls, we incubated cells with nocodazole (lanes 2 and 6) and doxorubicin (lanes 3 and 7), respectively. Doxorubicin is a genotoxic agent that intercalates into DNA, inhibits topoisomerase 2 and induces G_2 arrest via Cdc2 Tyr15 phosphorylation, without allowing mitotic entry. Nocodazole arrests cells in mitosis and exerts its effect by depolymerizing microtubules. HeLa cells transduced with pHR-VPR displayed a high level of H3 phosphorylation (lane 4), whereas transduced SupT1 cells displayed no detectable H3 phosphorylation (lane 8). Therefore, Vpr expression leads to mitotic entry in HeLa cells following G_2 arrest, whereas Vpr causes sustained G_2 arrest in SupT1 cells without subsequent mitotic entry.

Analysis of G_2 Arrest and Apoptosis Induction by Clinically Relevant Vpr Alleles and by a Vpr-GFP Fusion Chimera

Several natural or laboratory-constructed mutants of HIV-1 Vpr have been reported that selectively ablate either G_2 arrest or apoptosis. These mutants can be categorized into two groups. The first group includes *vpr* alleles with amino acid substitutions that have been observed in long-term nonprogressors, with a reduced ability to cause apoptosis but with normal induction of G_2 arrest. These substitutions include Q3R [22], R77Q [21], and I47A [58]. The second group includes Vpr-GFP and GFP-Vpr fusion proteins. In particular, it was reported that while a GFP-Vpr (whereby Vpr is

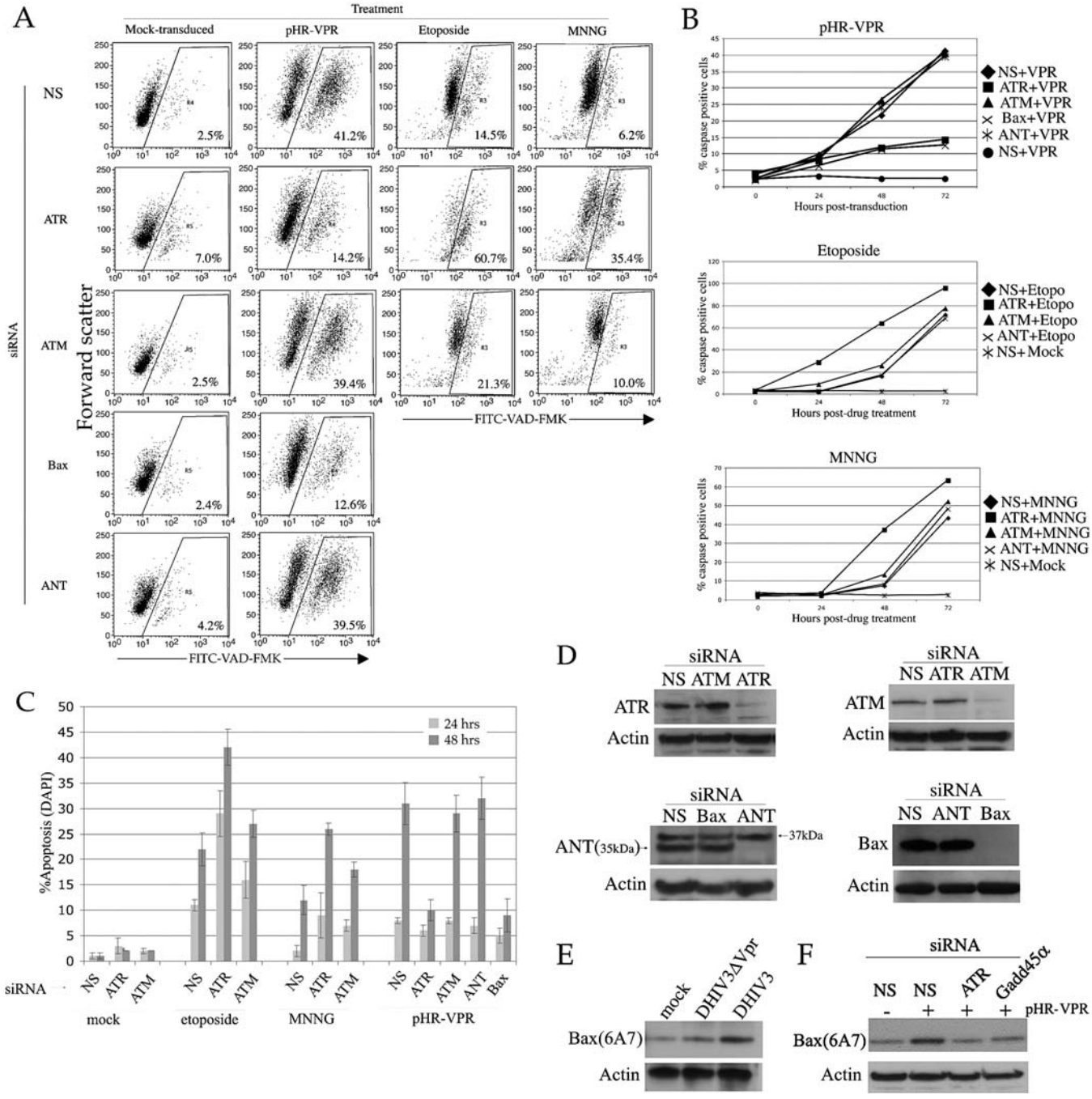

Figure 4. siRNA-Mediated Knockdown of ATR or Bax, but Not of ANT, Suppresses Vpr-Induced Apoptosis

(A) HeLa cells were transfected with nonspecific (NS) siRNA or siRNA targeted to ATR, or ATM as indicated. At 48 h post-transfection, cells were either treated with 25 μM etoposide, treated with 25 μM MNNG, mock-transduced, or transduced with pHR-VPR-R. Additionally, cells transfected with siRNAs targeted to Bax or ANT were transduced with pHR-VPR-R or mock-transduced (lower left dot plots). Cells from each treatment were assayed for caspase activity as in Figure 2B.

(B) Cells treated as in (A) were harvested at specified time points post-transduction and assayed for caspase activity.

(C) Cells treated as in (A) were stained with DAPI, and the results were quantified by microscopy.

(D) Cells treated with the indicated siRNAs were lysed and analyzed by Western blot to verify knockdown efficiency.

(E) Primary human $CD4^+$ lymphocytes were infected with DHIV3, infected with DHIV3ΔVPR, or mock-infected. At 48 h postinfection, cells in each treatment were lysed and assayed for protein concentration. Equal amounts of protein from each treatment were incubated with Bax6A7 monoclonal antibody. Antibody–protein complexes were precipitated with agarose beads and boiled and then subjected to Western blot analysis with a polyclonal antibody to Bax.

(F) HeLa cells treated with the indicated siRNAs and transduced with pHR-VPR or mock-transduced were lysed; reactivity to Bax6A7 antibody was assayed as described in (E).

doi:10.1371/journal.ppat.0020127.g004

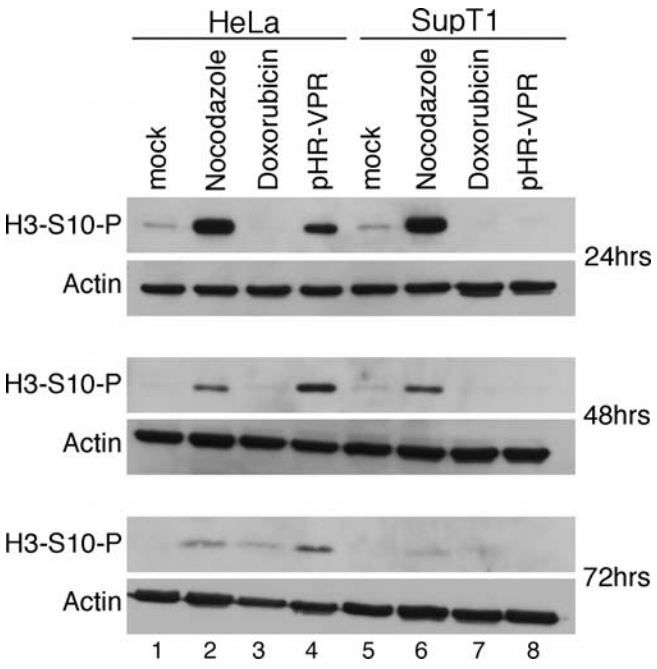

Figure 5. Vpr Induces Histone 3 Phosphorylation in HeLa but Not in SupT1 Cells

HeLa or Supt1 cells were transduced with pHR-VPR-G and at indicated time points, lysed, and analyzed by Western blot with a phospho-specific antibody that recognizes phosphorylation of H3 at serine-10. Nocodazole (250 ng/ml) and doxorubicin (1 μM) were used as positive and negative controls, respectively.

doi:10.1371/journal.ppat.0020127.g005

carboxyl-terminal to GFP) fusion protein was inactive in both G_2 arrest and apoptosis induction, the reciprocal chimera, Vpr-GFP, was able to induce apoptosis in the absence of G_2 arrest [59]. Collectively, the data obtained with both groups of mutants would appear to support that induction of G_2 arrest and apoptosis are independent, separable functions of Vpr. We wished to examine the phenotype of these mutants and chimeras using the experimental paradigms we described in Figure 1.

The Vpr mutants, R77Q and I74A, were separately constructed in the background of pHR-VPR-R (which encodes HIV-1_{NL4-3} *vpr*). Lentiviral vectors were then produced and used to infect target cells. Transduced cells were then evaluated for cell cycle stage at 48 h and for apoptosis at 72 h (Figure 6A). The levels of apoptosis, as judged by staining with FITC-VAD-FMK, were very similar between wild-type Vpr, Vpr(R77Q), and Vpr(I74A) and the levels of G_2 arrest were also similar. To more directly assess whether the frequencies of G_2 arrest and apoptosis correlated with each other, we calculated the ratio of cells in apoptosis over cells in G_2 for each mutant Vpr (% apoptotic cells/% cells in G_2/M [Apo/G_2M]). If a Vpr mutant induces normal levels of G_2 arrest, but reduced levels of apoptosis, then the Apo/G_2M ratio should decrease. The Apo/G_2M ratios were 0.83 for wild-type Vpr, 0.91 for Vpr(R77Q), and 0.92 for Vpr(I74A). Therefore, we conclude that neither of the Vpr mutants tested here resulted in lower levels of apoptosis induction, when compared to wild-type Vpr.

We previously demonstrated that Vpr induced phosphorylation BRCA1 at residue Ser1423 by the ATR kinase and that this phosphorylation correlated with induction of apoptosis [17]. To examine whether the Vpr mutants had a normal ability to induce BRCA1 phosphorylation, we performed Western blot on lysates from cells infected with the above lentiviral vectors. Wild-type Vpr and mutants were able to induce BRCA1 phosphorylation, and this phosphorylation was, in all three cases, ablated by treatment with caffeine (Figure 6B). Therefore, we were unable to find any detectable differences in the functions of Vpr(R77Q) or Vpr(I74A) when compared with Vpr(R77).

We then examined the phenotype of a Vpr-GFP fusion protein. It is well known that the addition of recombinant amino acid sequences as small as the influenza hemagglutinin tag at the carboxyl terminus of Vpr results in failure of Vpr to activate the G_2 checkpoint [25]. Carboxyl-terminal addition of larger fusion partners, such as luciferase [25] or GFP [59], also results in ablation of the G_2 arrest. Waldhuber et al. [59] found that carboxyl-terminal addition of GFP resulted in a Vpr chimera that was fully able to induce apoptosis. We constructed a Vpr-GFP chimera and observed that it was, as expected, unable to induce G_2 arrest (unpublished data). We then examined the induction of apoptosis by the fusion protein. To generate an appropriate control, we introduced the R80A mutation in the fusion construct, to generate Vpr(R80A)-GFP, and tested its ability to induce apoptosis (Figure 6C). Both Vpr-GFP and Vpr(R80A)-GFP were able to induce apoptosis. Since Vpr(R80A) that is not fused to GFP is unable to induce apoptosis (Figures 1 and 2), we expected that the introduction of the R80A substitution in the Vpr-GFP fusion protein [Vpr(R80A)-GFP] would also result in a protein devoid of apoptosis induction. Surprisingly, Vpr(R80A)-GFP is also capable of inducing apoptosis. Because the fusion with carboxyl-terminal GFP turns Vpr(R80A), a nonproaptotic protein, into an apoptotic one, it appears that the induction of apoptosis by Vpr-GFP represents a gain-of-function phenotype and is not representative of the biology of wild-type Vpr.

In conclusion, our results suggest that induction of G_2 arrest and apoptosis by HIV-1 Vpr are functionally interrelated and not genetically separable.

Discussion

The Functional Relationship between G_2 Arrest and Apoptosis

One gap in our current understanding of checkpoint signaling and apoptosis lies between the activation of nuclear checkpoint sentinels, such as ATR and ATM, and the involvement of Bcl-2 family of apoptosis regulators at the mitochondria. Previous reports have suggested that nuclear proteins, such as Rad9 or Histone H1, may translocate from the nucleus to the cytoplasm in response to DNA damage, to interact with mitochondrion-associated Bcl-2 family proteins and promote cytochrome *c* release and apoptosis [60,61]. In other instances of DNA damage, activated p53 was shown to directly promote Bax activation [62,63]. However, loss of p53 does not abrogate induction of apoptosis by Vpr [30,64], and we have been unable to observe Rad9 or histone H1 translocation to the mitochondria in response to Vpr (J. L. Andersen and V. Planelles, unpublished data). These observations, taken together with the results presented here, indicate that Vpr links checkpoint activation and apoptosis

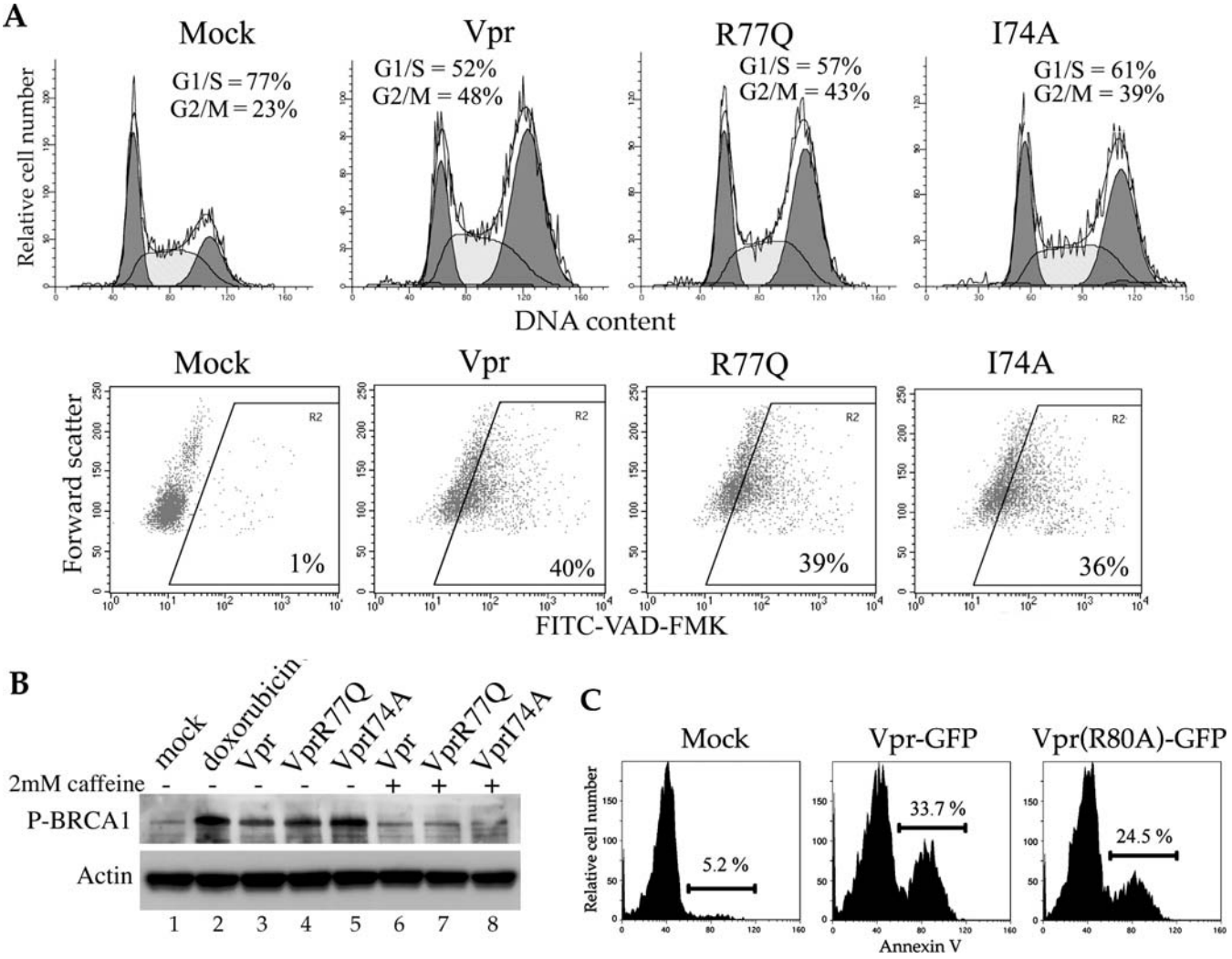

Figure 6. Functional Analysis of Vpr Mutants

(A) SupT1 cells were infected with pHR-VPR-R or indicated mutants, at an MOI of 0.5. At 48 h postinfection, cells were stained with hypotonic PI to determine the cell cycle profiles. At 72 h postinfection, cells were incubated with FITC-VAD-FMK and analyzed by flow cytometry to determine the percentage of cells with active caspases.

(B) Cells from above treatments were lysed at 48 h postinfection, and Western blot was performed to assay for phosphorylation of BRCA1 at Ser1423 by the ATR kinase. To establish the role of ATR in BRCA1 phosphorylation, parallel infections were treated with caffeine (2 mM).

(C) Induction of apoptosis by Vpr-GFP and Vpr(R80A)-GFP fusion proteins. HPB-ALL cells were transfected with indicated constructs or mock-transfected and 48 after transfection, phosphatidylserine exposure was analyzed by flow cytometry using phycoerythrin-conjugated annexin V.

doi:10.1371/journal.ppat.0020127.g006

in a novel manner and that a key element is the requirement for entry into G_2 (Figure 7A).

In support of a cause–effect relationship between Vpr-induced G_2 arrest and apoptosis, several reports demonstrate that the apoptotic effect of Vpr can be overridden by suppressing G_2-specific cell cycle–regulating kinases [17–20]. Yuan et al. [19,20] found that Wee1, a kinase which negatively regulates Cdk1 activity and thus regulates the G_2-to-M transition, is activated by Vpr. Furthermore, Yuan et al. [19,20] showed that suppression of Wee1 in the presence of Vpr abrogated both Vpr-induced G_2 arrest and apoptosis.

The Role of ATR in Vpr-Induced Apoptosis Differs from Its Role in Genotoxic Stress-Induced Apoptosis

We also demonstrate that ATR knockdown exacerbates genotoxin-induced apoptosis but, surprisingly, relieves Vpr-induced apoptosis [17]. The different effects of ATR knockdown on Vpr- versus genotoxin-induced apoptosis suggest that Vpr activity fundamentally differs from genotoxic stress. More specifically, it is tempting to speculate that such a difference resides in the fact that Vpr does not cause physical DNA damage (such as DSBs) whereas genotoxic agents do. In fact, three lines of evidence indicate that Vpr activates ATR in a manner that does not involve generation of DSBs: (1) Pulse-field gel electrophoresis revealed no DSBs in *vpr*-expressing cells [12]. (2) Vpr fails to induce phosphorylation of ATM at serine-1981, a residue linked to DSB signaling and potently phosphorylated in response to ionizing radiation [12]. (3) And, as we have shown here, in contrast with etoposide-induced apoptosis, Vpr-induced apoptosis is relieved under conditions of checkpoint suppression.

Models for Vpr activity that would be in agreement with

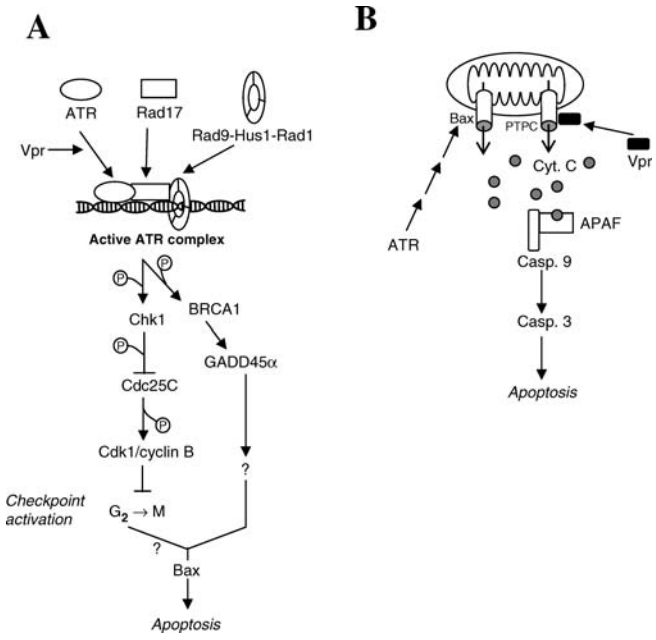

Figure 7. Models to Explain the Activities of HIV-1 Vpr

(A). Activation of ATR by Vpr and downstream signaling consequences leading to both G_2 arrest and apoptosis. The functional link between GADD45α and activation of Bax and the mechanism by which G_2 arrest leads to Bax activation remain unknown (question marks).

(B) Binding of Vpr to mitochondrial PTPC was proposed to trigger release of cytochrome *c* and induction of apoptosis, independently of cell cycle status; in this work, we propose that an alternative pore-forming mitochondrial protein, Bax, is the effector of Vpr-induced apoptosis, and that Bax activation requires upstream stress signals derived from ATR.

doi:10.1371/journal.ppat.0020127.g007

the lack of DSB formation by Vpr have been proposed in the past. For example, Vpr may perturb nuclear envelope integrity, as suggested by de Noronha et al. [65]. Perturbation of nuclear envelope integrity may, in turn, lead to ATR activation. In addition, Lai et al. proposed that Vpr binds directly to chromatin in a manner that results in ATR activation [12].

Role of the Mitochondria in Vpr-Induced Apoptosis

Previous reports have suggested that Vpr induces apoptosis via a direct interaction with ANT at the inner mitochondrial membrane, which results in release of cytochrome *c* from fractionated mitochondria [23]. These observations would indicate that Vpr induces mitochondrial depolarization directly, rather than activating upstream stress signals, and suggest that Vpr may induce apoptosis rapidly after being expressed (Figure 7B). We reasoned that if Vpr induced apoptosis by interacting directly with the mitochondria, it would efficiently induce apoptosis regardless of cell cycle status. In contrast with the previous expectation, we observed that cell cycle transition into G_2 is required for Vpr to induce apoptosis. Furthermore, blockade of the cell cycle in G_1 for 48 h effectively prevented apoptosis, and subsequent release of the block allowed apoptosis induction, coinciding with entry into G_2.

Jacotot et al. [23] proposed that the mitochondrial channel activated by Vpr is the PTPC. In sharp contrast, we find that efficient removal of ANT (an essential domain of PTPC) did not affect Vpr apoptosis to any degree. Instead, removal of Bax, an independent mitochondrial pore-forming protein, led to nearly complete suppression of apoptosis. Furthermore, Bax activation is dependent on the presence of ATR, as is induction of apoptosis. Taken together, our data strongly support a model in which the apical step toward Vpr-induced apoptosis is activation of ATR, followed by the activation of downstream apoptotic mediators such as Bax, Smac, and caspases (Figure 7).

Role of Vpr in HIV-1 Pathogenesis

Depletion of $CD4^+$ lymphocytes due to HIV-1 infection leads to immune suppression in AIDS patients (reviewed in [66]). The cause of T-cell depletion in AIDS patients is a question under intense research but remains poorly understood. The discovery of mutations in Vpr that may be associated with long-term nonprogressors and impair the apoptosis-inducing ability of Vpr suggests a critical role for Vpr in AIDS pathology [21,22,58]. However, for the Vpr mutation, R77Q, a recent report has questioned its association with long-term nonprogressors [67]. Fisher et al. [67] proposed that R77Q is associated with certain viral subtypes, such as subtype A, and not with disease progression. A more recent analysis of the GenBank database revealed that R77 predominates in subtype B, whereas Q77 predominates in clades A, C, D, G, and H and groups O and N viruses, and subtype F and K strains frequently encode H77 [68]. Rajan et al. [68] also reported, using isogenic, full-length viruses, that HIV-1 carrying Q77 displayed reduced cytopathicity if the virus had R5 tropism but not if it had X4 tropism. The previous experiments did not uncouple the cytopathic potential of the virus strains from their replication kinetics. Therefore, in our studies, we wished to examine the proapoptotic potential of mutant Vpr proteins in the context of a nonreplicating lentiviral vector and in the absence of other viral genes. Our results conclusively show that in our experimental paradigm, the proapoptotic potentials of Vpr(R77Q) and Vpr(I74A) are indistinguishable from that of Vpr(R77). Thus, the results by Rajan et al. [68] would seem to indicate that the R77Q substitution has a moderate, positive effect on cell viability, and this effect may be related to viral replication efficiency rather than to proapoptotic signaling.

Materials and Methods

Western blotting procedures. For PARP and HA-Vpr detection, cells were detached with trypsin, washed once with media containing 10% fetal bovine serum, and then washed twice in PBS. Detached cells were pelleted by centrifugation and then resuspended in ice-cold lysis buffer (20 mM Tris [pH 7.5], 100 mM NaCl, 0.5% NP-40, 0.5 mM EDTA) in the presence of Complete Protease Inhibitors (Roche, http://www.roche.com). Cell lysates were passed through a 25-gauge needle ten times and then resuspended in Criterion loading buffer (Bio-Rad, http://www.bio-rad.com). Next, 20 μg of cell lysate per sample was loaded on a Criterion XT 10% polyacrylamide gel (Bio-Rad). Following electrophoresis (at 50 amps/gel), proteins were transferred to Immobilon FL PVDF membranes (Millipore, http://www.millipore.com) and then immunostained with anti-PARP (Cell Signaling Technologies, http://www.cellsignal.com) and anti-rabbit 680 (Invitrogen, http://www.invitrogen.com) antibodies. The primary anti-PARP antibody was diluted 1:1,000 in TPBS (PBS, 0.1% Triton-X 100) plus 5% nonfat dry milk (NFDM). The secondary anti-rabbit 680 antibody was diluted 1:10,000 in TPBS plus 5% NFDM and 0.1% sodium dodecyl sulfate (SDS). Blots were incubated with secondary antibody for 1 h at 4 °C and then washed 5 times with TPBS. Protein bands were visualized by the Odyssey infrared system (LI-COR Biosciences, http://www.licor.com). Protein concentrations of all samples were determined by BCA protein assay (Pierce Biotechnology, http://www.piercenet.com) prior to loading.

For all other Western blots, the above protocol was followed with

the exception that secondary HRP-conjugated antibodies were diluted in TPBS plus 5% NFDM and bands were visualized by ECL detection, using ECL plus (Amersham Biosciences, http://www.amersham.com). For Bax 6A7 immunoprecipitation, cells were lysed in CHAPS buffer (10 mM HEPES, 150 mM NaCl, 1% CHAPS, protease inhibitors) on ice for 10 min, followed by ten passes through a 25-gauge needle. Then, 2 μg of Bax 6A7 monoclonal antibody (Abcam, http://www.abcam.com) was added to 1 mg of cellular protein and incubated 8 h at 4 °C under constant mixing followed by incubation with protein A/G beads (Santa Cruz Biotechnology, http://www.scbt.com) according to the manufacturer's protocol. Protein–bead complexes were then washed with lysis buffer 3 times, boiled for 3 min, and subject to Western blot with anti-Bax antibody (Cell Signaling Technologies) and ECL detection according to methods described above. Antibodies used were anti-ATR (obtained from Dr. Paul Nghiem, Harvard University, Boston, Massachusetts, United States), anti-GADD45 (Santa Cruz Biotechnology), anti-Bax (Cell Signaling Technologies), anti–cytochrome *c* (Santa Cruz Biotechnology), anti-Smac/Diablo (Imgenex Corporation, http://www.imgenex.com), and Bax 6A7 (Abcam).

Cell cycle analysis. Cells were harvested and counted; 1×10^6 cells were aliquoted into tubes and washed once with cold PBS. Washed cells were resuspended in 0.5 ml of cold PBS, following which 2 ml of ice-cold ethanol was slowly added with gently vortexing. Ethanol-fixed cells were left overnight at −20 °C. The following day, cells were centrifuged at $828 \times g$, and ethanol was washed from the cells. Cells were then resuspended in propidium iodide staining buffer (10 μg/ml propidium iodide, 2% FBS, 11.25 kU RNase A/ml, 0.02% sodium azide) and allowed to incubate for 10 min on ice prior to analysis of DNA content by flow cytometry. Cell cycle profiles were further analyzed using Modfit software (Verity Software, http://www.vsh.com) to derive percentages of cells in different phases of cell cycle.

Viral vectors and virus. DHIV3 and pHR lentiviral vectors were produced by transient transfection of HEK293T cells. For production of pHR vectors, pHR-VPR or pHR-VPR(R80A) was cotransfected with pCMVΔR8.2ΔVPR [69], and pHCMV-VSVG [70] by calcium phosphate–mediated transfection [18]. Virus-containing supernatants were harvested at 24, 48, and 72 h post-transfection. Supernatants were cleared of cellular debris by centrifugation at $828 \times g$ for 10 min, and virus in cleared supernatants was concentrated by centrifugation at $115{,}889 \times g$ for 2 h at 4 °C. Virus was titered by infection of HeLa cells and subsequent flow cytometric analysis of the reporter molecule GFP. Vector titers were calculated with the equation $[(F \times C_0)/V] \times D$, where F is the frequency of GFP-positive cells found by flow cytometry, C_0 is the total number of target cells at the time of infection, V is the volume of inoculum, and D is the virus dilution factor. The virus dilution factor used for titrations was 10. The total number of target cells at the time of infection for titer was 0.5×10^6. Infections were performed at a multiplicity of infection (MOI) of 2.5 with 10 μg of Polybrene/ml for 8 h. Infections of siRNA-treated cells were performed 48 h after siRNA transfection. T cells and HeLa cells were transduced with virus diluted in cell culture media with 8 μg/ml and 10 μg/ml Polybrene, respectively. For HeLa cell transduction, virus-containing media was washed after 8 h and replaced with fresh culture media. T cells were transduced by spinoculation as previously described [71].

The HIV-1 molecular clone HIV-1_{NL4-3} was transfected into 2×10^7 HEK293FT cells by calcium phosphate transfection. At 48 h after transfection, HEK293FT cells were co-cultured with 10^7 MT-2 cells for 5 h. MT-2 cells were then cultured alone until approximately 75% of cell clumps showed syncitia. Virus-containing supernatants were then cleared of cells and debris by centrifugation at 2,000 rpm for 10 min. Viral stocks were then frozen at −80 °C. Spin infections were performed as described above.

Apoptosis assays. For analysis of apoptotic nuclear morphology, cells were fixed in the well with 2% paraformaldehyde (in PBS) for 15 min at room temperature (RT). Fixed cells were then permeabilized in 0.1% Triton X-100 (in PBS) for 15 min at RT, gently washed 2 times in PBS, and then incubated in 0.5 μg/ml DAPI (Invitrogen) for 45 min at 37 °C. Apoptotic nuclei were identified by fluorescence microscopy, counted, and divided by total cells in the field to determine percent apoptosis. For cell counting, fields were chosen at random, and a minimum of 1,000 cells were counted per treatment in each experiment. Standard deviations were derived from three separate experiments. PARP cleavage was assayed by Western blot as described above. For analysis of caspase activity, cells were stained with FITC-VAD-FMK (Promega, http://www.promega.com) or RED-VAD-FMK (Calbiochem/EMD Biosciences, http://www.emdbiosciences.com) according to manufacturer's protocols. Caspase-stained cells were analyzed by flow cytometry.

Phosphatidylserine exposure at the cell surface was analyzed as previously described [72] by flow cytometry using phycoerythrin-conjugated annexin V (Annexin V-PE, Bender MedSystems, http://www.bendermedsystems.com).

siRNA treatments. All siRNA treatments were performed with Dharmacon anti-human smart pool siRNA duplexes (Dharmacon, http://www.dharmacon.com). Smart pool siRNAs were transfected at a final concentration of 100 nM into exponentially growing HeLa cells with Oligofectamine (Invitrogen) according to the manufacturer's protocol. Cells were split 1:3 at 24 h post-transfection. At 48 h post-transfection, cells were harvested to verify knockdown by Western blot or subject to experimental treatments.

Cell culture. For experiments in which cell synchronization or the use of siRNAs was to be employed, we used the human cervical cancer cell line HeLa, which was maintained in Dulbecco's modified Eagle's medium (Cambrex BioScience (formerly BioWhittaker), http://www.cambrex.com), supplemented with 10% FCS and 2 mM L-glutamine. For experiments in which viral transduction and measurement of cell cycle/apoptosis were the aims, we used the human T-cell line SupT1, which was maintained in RPMI 1640 (Cambrex BioScience), supplemented with 10% FCS and L-glutamine.

Peripheral blood mononuclear cells were obtained with Leukopaks from unidentified, healthy donors (American Red Cross, http://www.redcross.org), and $CD4^+$ lymphocytes were purified using anti-CD4 magnetic beads (Dynal/Invitrogen) according to the manufacturer's instructions. $CD4^+$ T cells were activated by culture in RPMI plus 10% FBS plus 1 mM L-glutamine with 3 anti-CD3/anti-CD28 beads per cell (Invitrogen) for 2 d, changing medium daily. After 2 d, recombinant interleukin 2 was added to the culture medium at a concentration of 100 units/ml.

Drug treatments. Thymidine was diluted to a concentration of 2 mM in culture media and then added to exponentially growing HeLa cells. For experiments in which thymidine treatment was combined with viral gene expression, thymidine-containing media was added immediately following transduction. For experiments in which thymidine treatment was combined with genotoxic drugs, cells were incubated in thymidine-containing media for 4 h prior to the addition of genotoxins. Etoposide (Sigma Aldrich, http://www.signaaldrich.com) and MNNG (Sigma Aldrich) were diluted in culture media to a concentration of 25 μM and incubated with cells for 3 h. Following incubation, genotoxin-containing media was removed and replaced with fresh media with or without thymidine.

Supporting Information

Accession Numbers

The GenBank (http://www.ncbi.nlm.nih.gov/Genbank) accession numbers for the proteins discussed in this paper are ANT (P12235 [GenPept]), ATM (NM__000051), ATR (NM__001184), BRCA1 (NP__009233), GADD45α (NM__001924), HIV-1_{NL4-3} VPR (AAB60574 [GenPept]), and VDAC (P21796 [GenPept]).

Acknowledgments

We thank Dr. Wayne Green, Dr. Douglas Grossman, Namson Hawk, and Michael Blackwell for technical assistance and Dr. Christopher D. Freel for insight into potential Vpr interactions. We are grateful to Dr. Paul Nghiem for providing antibodies to ATR.

Author contributions. JLA, GJ, SB, and VP conceived and designed the experiments. JLA, JLD, GJ, and SB performed the experiments. JLA, JLD, GJ, SB, and VP analyzed the data. JLA, JLD, ESZ, OA, BK, and VP contributed reagents/materials/analysis tools. JLA and VP wrote the paper.

Funding. This research was supported by National Institutes of Health (NIH) research grant AI49057 to VP. JLA is supported by NIH Training Grant in Microbial Pathogenesis T32 AI055434. ESZ is supported by NIH Genetics Training Grant T32 GM07464.

Competing interests. The authors have declared that no competing interests exist.

References

1. Derdeyn CA, Silvestri G (2005) Viral and host factors in the pathogenesis of HIV infection. Curr Opin Immunol 17: 366–373.
2. Gougeon ML (2003) Apoptosis as an HIV strategy to escape immune attack. Nat Rev Immunol 3: 392–404.
3. Roshal M, Zhu Y, Planelles V (2001) Apoptosis in AIDS. Apoptosis 6: 103–116.
4. Haase AT (1999) Population biology of HIV-1 infection: Viral and CD4+ T cell demographics and dynamics in lymphatic tissues. Annu Rev Immunol 17: 625–656.
5. Perelson AS, Neumann AU, Markowitz M, Leonard JM, Ho DD (1996) HIV-1 dynamics in vivo: Virion clearance rate, infected cell life-span, and viral generation time. Science 271: 1582–1586.
6. Wei X, Ghosh SK, Taylor ME, Johnson VA, Emini EA, et al. (1995) Viral dynamics in human immunodeficiency virus type 1 infection. Nature 373: 117–122.
7. Simon V, Ho DD (2003) HIV-1 dynamics in vivo: Implications for therapy. Nat Rev Microbiol 1: 181–190.
8. Andersen JL, Planelles V (2005) The role of Vpr in HIV-1 pathogenesis. Curr HIV Res 3: 43–51.
9. Le Rouzic E, Benichou S (2005) The Vpr protein from HIV-1: Distinct roles along the viral life cycle. Retrovirology 2: 11.
10. Muthumani K, Zhang D, Hwang DS, Kudchodkar S, Dayes NS, et al. (2002) Adenovirus encoding HIV-1 Vpr activates caspase 9 and induces apoptotic cell death in both p53 positive and negative human tumor cell lines. Oncogene 21: 4613–4625.
11. Muthumani K, Hwang DS, Desai BM, Zhang D, Dayes N, et al. (2002) HIV-1 Vpr induces apoptosis through caspase 9 in T cells and peripheral blood mononuclear cells. J Biol Chem 277: 37820–37831.
12. Lai M, Zimmerman ES, Planelles V, Chen J (2005) Activation of the ATR pathway by human immunodeficiency virus type 1 Vpr involves its direct binding to chromatin in vivo. J Virol 79: 15443–15451.
13. Roshal M, Kim B, Zhu Y, Nghiem P, Planelles V (2003) Activation of the ATR-mediated DNA damage response by the HIV-1 viral protein R. J Biol Chem 278: 25879–25886.
14. Zimmerman ES, Chen J, Andersen JL, Ardon O, Dehart JL, et al. (2004) Human immunodeficiency virus type 1 Vpr-mediated G2 arrest requires Rad17 and Hus1 and induces nuclear BRCA1 and γ-H2AX focus formation. Mol Cell Biol 24: 9286–9294.
15. Bao S, Tibbetts RS, Brumbaugh KM, Fang Y, Richardson DA, et al. (2001) ATR/ATM-mediated phosphorylation of human Rad17 is required for genotoxic stress responses. Nature 411: 969–974.
16. Zou L, Cortez D, Elledge SJ (2002) Regulation of ATR substrate selection by Rad17-dependent loading of Rad9 complexes onto chromatin. Genes Dev 16: 198–208.
17. Andersen JL, Zimmerman ES, Dehart JL, Murala S, Ardon O, et al. (2005) ATR and GADD45alpha mediate HIV-1 Vpr-induced apoptosis. Cell Death Differ 12: 326–334.
18. Zhu Y, Gelbard HA, Roshal M, Pursell S, Jamieson BD, et al. (2001) Comparison of cell cycle arrest, transactivation, and apoptosis induced by the simian immunodeficiency virus SIVagm and human immunodeficiency virus type 1 vpr genes. J Virol 75: 3791–3801.
19. Yuan H, Kamata M, Xie YM, Chen IS (2004) Increased levels of Wee-1 kinase in G(2) are necessary for Vpr- and gamma irradiation-induced G(2) arrest. J Virol 78: 8183–8190.
20. Yuan H, Xie YM, Chen IS (2003) Depletion of Wee-1 kinase is necessary for both human immunodeficiency virus type 1 Vpr- and gamma irradiation-induced apoptosis. J Virol 77: 2063–2070.
21. Lum JJ, Cohen OJ, Nie Z, Weaver JG, Gomez TS, et al. (2003) Vpr R77Q is associated with long-term nonprogressive HIV infection and impaired induction of apoptosis. J Clin Invest 111: 1547–1554.
22. Somasundaran M, Sharkey M, Brichacek B, Luzuriaga K, Emerman M, et al. (2002) Evidence for a cytopathogenicity determinant in HIV-1 Vpr. Proc Natl Acad Sci U S A 99: 9503–9508.
23. Jacotot E, Ravagnan L, Loeffler M, Ferri KF, Vieira HL, et al. (2000) The HIV-1 viral protein R induces apoptosis via a direct effect on the mitochondrial permeability transition pore. J Exp Med 191: 33–46.
24. Vieira HL, Haouzi D, El Hamel C, Jacotot E, Belzacq AS, et al. (2000) Permeabilization of the mitochondrial inner membrane during apoptosis: Impact of the adenine nucleotide translocator. Cell Death Differ 7: 1146–1154.
25. Di Marzio P, Choe S, Ebright M, Knoblauch R, Landau NR (1995) Mutational analysis of cell cycle arrest, nuclear localization and virion packaging of human immunodeficiency virus type 1 Vpr. J Virol 69: 7909–7916.
26. Zimmerman ES, Sherman MP, Blackett JL, Neidleman JA, Kreis C, et al. (2006) HIV-1 Vpr induces DNA replication stress in vitro and in vivo. J Virol 80: 10407–10418.
27. Gaynor EM, Chen IS (2001) Analysis of apoptosis induced by HIV-1 Vpr and examination of the possible role of the hHR23A protein. Exp Cell Res 267: 243–257.
28. Firket H, Mahieu P (1967) Synchronization of division induced in HeLa cells with an excess of thymidine. Studies on blockage of various stages of the cell cycle. Exp Cell Res 45: 11–22.
29. Ardon O, Zimmerman ES, Andersen JL, DeHart JL, Blackett J, et al. (2006) Induction of G2 arrest and binding to cyclophilin A are independent phenotypes of human immunodeficiency virus type 1 Vpr. J Virol 80: 3694–3700.
30. Shostak LD, Ludlow J, Fisk J, Pursell S, Rimel BJ, et al. (1999) Roles of p53 and caspases in the induction of cell cycle arrest and apoptosis by HIV-1 vpr. Exp Cell Res 251: 156–165.
31. Stojic L, Mojas N, Cejka P, Di Pietro M, Ferrari S, et al. (2004) Mismatch repair-dependent G2 checkpoint induced by low doses of SN1 type methylating agents requires the ATR kinase. Genes Dev 18: 1331–1344.
32. Clifford B, Beljin M, Stark GR, Taylor WR (2003) G2 arrest in response to topoisomerase II inhibitors: The role of p53. Cancer Res 63: 4074–4081.
33. Poon B, Jowett JB, Stewart SA, Armstrong RW, Rishton GM, et al. (1997) Human immunodeficiency virus type 1 vpr gene induces phenotypic effects similar to those of the DNA alkylating agent, nitrogen mustard. J Virol 71: 3961–3971.
34. Hammond EM, Dorie MJ, Giaccia AJ (2004) Inhibition of ATR leads to increased sensitivity to hypoxia/reoxygenation. Cancer Res 64: 6556–6562.
35. Castedo M, Perfettini JL, Roumier T, Andreau K, Medema R, et al. (2004) Cell death by mitotic catastrophe: A molecular definition. Oncogene 23: 2825–2837.
36. Yu Q, La Rose J, Zhang H, Takemura H, Kohn KW, et al. (2002) UCN-01 inhibits p53 up-regulation and abrogates gamma-radiation-induced G(2)-M checkpoint independently of p53 by targeting both of the checkpoint kinases, Chk2 and Chk1. Cancer Res 62: 5743–5748.
37. Truman JP, Gueven N, Lavin M, Leibel S, Kolesnick R, et al. (2005) Down-regulation of ATM protein sensitizes human prostate cancer cells to radiation-induced apoptosis. J Biol Chem 280: 23262–23272.
38. Verrier F, Mignotte B, Jan G, Brenner C (2003) Study of PTPC composition during apoptosis for identification of viral protein target. Ann N Y Acad Sci 1010: 126–142.
39. Kokoszka JE, Waymire KG, Levy SE, Sligh JE, Cai J, et al. (2004) The ADP/ATP translocator is not essential for the mitochondrial permeability transition pore. Nature 427: 461–465.
40. Baines CP, Kaiser RA, Purcell NH, Blair NS, Osinska H, et al. (2005) Loss of cyclophilin D reveals a critical role for mitochondrial permeability transition in cell death. Nature 434: 658–662.
41. Li Y, Johnson N, Capano M, Edwards M, Crompton M (2004) Cyclophilin-D promotes the mitochondrial permeability transition but has opposite effects on apoptosis and necrosis. Biochem J 383: 101–109.
42. Nakagawa T, Shimizu S, Watanabe T, Yamaguchi O, Otsu K, et al. (2005) Cyclophilin D-dependent mitochondrial permeability transition regulates some necrotic but not apoptotic cell death. Nature 434: 652–658.
43. Antonsson B, Montessuit S, Sanchez B, Martinou JC (2001) Bax is present as a high molecular weight oligomer/complex in the mitochondrial membrane of apoptotic cells. J Biol Chem 276: 11615–11623.
44. Norbury CJ, Zhivotovsky B (2004) DNA damage-induced apoptosis. Oncogene 23: 2797–2808.
45. Cory S, Huang DC, Adams JM (2003) The Bcl-2 family: Roles in cell survival and oncogenesis. Oncogene 22: 8590–8607.
46. Kuwana T, Mackey MR, Perkins G, Ellisman MH, Latterich M, et al. (2002) Bid, Bax, and lipids cooperate to form supramolecular openings in the outer mitochondrial membrane. Cell 111: 331–342.
47. Rostovtseva TK, Antonsson B, Suzuki M, Youle RJ, Colombini M, et al. (2004) Bid, but not Bax, regulates VDAC channels. J Biol Chem 279: 13575–13583.
48. Annis MG, Soucie EL, Dlugosz PJ, Cruz-Aguado JA, Penn LZ, et al. (2005) Bax forms multispanning monomers that oligomerize to permeabilize membranes during apoptosis. EMBO J 24: 2096–2103.
49. Rathmell JC, Fox CJ, Plas DR, Hammerman PS, Cinalli RM, et al. (2003) Akt-directed glucose metabolism can prevent Bax conformation change and promote growth factor-independent survival. Mol Cell Biol 23: 7315–7328.
50. He J, Choe S, Walker R, Di Marzio P, Morgan DO, et al. (1995) Human immunodeficiency virus type 1 viral protein R (Vpr) arrests cells in the G2 phase of the cell cycle by inhibiting p34cdc2 activity. J Virol 69: 6705–6711.
51. Jowett JB, Planelles V, Poon B, Shah NP, Chen ML, et al. (1995) The human immunodeficiency virus type 1 vpr gene arrests infected T cells in the G2 + M phase of the cell cycle. J Virol 69: 6304–6313.
52. Re F, Braaten D, Franke EK, Luban J (1995) Human immunodeficiency virus type 1 Vpr arrests the cell cycle in G2 by inhibiting the activation of p34cdc2-cyclin B. J Virol 69: 6859–6864.
53. Bartz SR, Rogel ME, Emerman M (1996) Human immunodeficiency virus type 1 cell cycle control: Vpr is cytostatic and mediates G2 accumulation by a mechanism which differs from DNA damage checkpoint control. J Virol 70: 2324–2331.
54. Chang F, Re F, Sebastian S, Sazer S, Luban J (2004) HIV-1 Vpr induces defects in mitosis, cytokinesis, nuclear structure, and centrosomes. Mol Biol Cell 15: 1793–1801.
55. Watanabe N, Yamaguchi T, Akimoto Y, Rattner JB, Hirano H, et al. (2000) Induction of M-phase arrest and apoptosis after HIV-1 Vpr expression through uncoupling of nuclear and centrosomal cycle in HeLa cells. Exp Cell Res 258: 261–269.
56. Hendzel MJ, Wei Y, Mancini MA, Van Hooser A, Ranalli T, et al. (1997) Mitosis-specific phosphorylation of histone H3 initiates primarily within pericentromeric heterochromatin during G2 and spreads in an ordered

fashion coincident with mitotic chromosome condensation. Chromosoma 106: 348–360.
57. Juan G, Traganos F, James WM, Ray JM, Roberge M, et al. (1998) Histone H3 phosphorylation and expression of cyclins A and B1 measured in individual cells during their progression through G2 and mitosis. Cytometry 32: 71–77.
58. Zhao Y, Chen M, Wang B, Yang J, Elder RT, et al. (2002) Functional conservation of HIV-1 Vpr and variability in a mother-child pair of long-term non-progressors. Virus Res 89: 103–121.
59. Waldhuber MG, Bateson M, Tan J, Greenway AL, McPhee DA (2003) Studies with GFP-Vpr fusion proteins: Induction of apoptosis but ablation of cell-cycle arrest despite nuclear membrane or nuclear localization. Virology 313: 91–104.
60. Konishi A, Shimizu S, Hirota J, Takao T, Fan Y, et al. (2003) Involvement of histone H1.2 in apoptosis induced by DNA double-strand breaks. Cell 114: 673–688.
61. Ishii H, Inageta T, Mimori K, Saito T, Sasaki H, et al. (2005) Frag1, a homolog of alternative replication factor C subunits, links replication stress surveillance with apoptosis. Proc Natl Acad Sci U S A 102: 9655–9660.
62. Chipuk JE, Bouchier-Hayes L, Kuwana T, Newmeyer DD, Green DR (2005) PUMA couples the nuclear and cytoplasmic proapoptotic function of p53. Science 309: 1732–1735.
63. Chipuk JE, Kuwana T, Bouchier-Hayes L, Droin NM, Newmeyer DD, et al. (2004) Direct activation of Bax by p53 mediates mitochondrial membrane permeabilization and apoptosis. Science 303: 1010–1014.
64. Stewart SA, Poon B, Jowett JB, Xie Y, Chen IS (1999) Lentiviral delivery of HIV-1 Vpr protein induces apoptosis in transformed cells. Proc Natl Acad Sci U S A 96: 12039–12043.
65. de Noronha CM, Sherman MP, Lin HW, Cavrois MV, Moir RD, et al. (2001) Dynamic disruptions in nuclear envelope architecture and integrity induced by HIV-1 Vpr. Science 294: 1105–1108.
66. Hazenberg MD, Hamann D, Schuitemaker H, Miedema F (2000) T cell depletion in HIV-1 infection: how CD4+ T cells go out of stock. Nat Immunol 1: 285–289.
67. Fischer A, Lejczak C, Lambert C, Roman F, Servais J, et al. (2004) Is the Vpr R77Q mutation associated with long-term non-progression of HIV infection? AIDS 18: 1346–1347.
68. Rajan D, Wildum S, Rucker E, Schindler M, Kirchhoff F (2006) Effect of R77Q, R77A and R80A changes in Vpr on HIV-1 replication and CD4 T cell depletion in human lymphoid tissue ex vivo. AIDS 20: 831–836.
69. An DS, Morizono K, Li QX, Mao SH, Lu S, et al. (1999) An inducible human immunodeficiency virus type 1 (HIV-1) vector which effectively suppresses HIV-1 replication. J Virol 73: 7671–7677.
70. Akkina RK, Walton RM, Chen ML, Li QX, Planelles V, et al. (1996) High-efficiency gene transfer into CD34+ cells with a human immunodeficiency virus type 1-based retroviral vector pseudotyped with vesicular stomatitis virus envelope glycoprotein G. J Virol 70: 2581–2585.
71. O'Doherty U, Swiggard WJ, Malim MH (2000) Human immunodeficiency virus type 1 spinoculation enhances infection through virus binding. *J Virol* 74: 10074–10080.
72. Py B, Slomianny C, Auberger P, Petit PX, Benichou S (2004) Siva-1 and an alternative splice form lacking the death domain, Siva-2, similarly induce apoptosis in T lymphocytes via a caspase-dependent mitochondrial pathway. J Immunol 172: 4008–4017.